

Article

# Exploring Multi-Scale Spatiotemporal Twitter User Mobility Patterns with a Visual-Analytics Approach

Junjun Yin <sup>1</sup> and Zhenhong Du <sup>2,\*</sup>

<sup>1</sup> Department of Geography and Geographic Information Science, University of Illinois at Urbana-Champaign, Urbana, IL 61801, USA; jyn@illinois.edu

<sup>2</sup> Key Laboratory of Geographic Information Science, School of Earth Sciences, Zhejiang University, Hangzhou, 310028, China; duzhenhong@zju.edu.cn

\* Correspondence: duzhenhong@zju.edu.cn; Tel.: +8613819192989

Academic Editor: name

Version September 19, 2016 submitted to ISPRS Int. J. Geo-Inf.; Typeset by LATEX using class file mdpi.cls

**Abstract:** Understanding human mobility patterns is of great importance for urban planning, traffic management, and even marketing campaign. However, the capability of capturing detailed human movements with fine-grained spatial and temporal granularity is still limited. In this study, we extracted high-resolution mobility data from a collection of over 1.3 billion geo-located Twitter messages. Regarding the concerns of infringement on individual privacy, such as the mobile phone call records with restricted access, the dataset is collected from publicly accessible Twitter data streams. In this paper, we employed a visual-analytics approach to studying multi-scale spatiotemporal Twitter user mobility patterns in the contiguous United States during the year 2014. Our approach included a scalable visual-analytics framework to deliver efficiency and scalability in filtering large volume of geo-located tweets, modeling and extracting Twitter user movements, generating space-time user trajectories, and summarizing multi-scale spatiotemporal user mobility patterns. We performed a set of statistical analysis to understand Twitter user mobility patterns across multi-level spatial scales and temporal ranges. In particular, Twitter user mobility patterns measured by the displacements and radius of gyration of individuals revealed multi-scale or multi-modal Twitter user mobility patterns. By further studying such mobility patterns in different temporal ranges, we identified both consistency and seasonal fluctuations regarding the distance decay effects in the corresponding mobility patterns. At the same time, our approach provides a geo-visualization unit with an interactive 3D virtual globe web mapping interface for exploratory geo-visual analytics of the multi-level spatiotemporal Twitter user movements.

**Keywords:** Geo-located tweets, mobility patterns, multi-scale spatiotemporal analysis, scalable visual-analytics framework

## 1. Introduction

Understanding human mobility patterns is of great importance for a broad range of applications from urban planning [1], traffic management [2], and even the spatial spread of epidemic diseases [3]. Earlier research efforts relied on low-resolution mobility data to understand human mobility patterns, such as using census records to study human migration patterns [4], or delivering questionnaires and asking volunteers to report the track of bank notes to infer human travel patterns [5]. However, such mobility data do not provide detailed human movements with fine-grained spatial and temporal granularity, which are usually aggregated and therefore are limited to capture mobility patterns of individuals [6,7]. In addition to the mobility data collected by GPS trackers [1,8] and mobile phone call records [6,9,10], emerging as a new mobility data source, today's pervasive Location Based Social

32 Media (LBSM) platforms (e.g., Twitter and Foursquare) offer continuous spatial Big Data streams with  
33 massive amount of detailed and frequently updated user digital footprints in the form of real-world  
34 user trails and footprints [11]. A significant advantage of utilizing LBSM data streams as proxies  
35 for studying human mobility patterns is the large spatial coverage. For instance, researchers have  
36 used geo-located tweets for studying global mobility patterns [12], which is otherwise impossible for  
37 other mobility datasets (e.g., GPS traces and mobile phone call records). Regarding the concerns of  
38 infringement on individual privacy, such as the mobile phone call records with restricted access [7,13,  
39 14], the publicly available LBSM data streams offer unique opportunities for conducting reproducible  
40 and comparative scientific findings across different geographic regions.

41 Many recent studies have adopted LBSM data streams to study human mobility patterns. For  
42 example, they modeled and extracted trajectories of individuals and performed statistical analysis  
43 focusing on the distance decay effects in the collective user movements [6], which were used to  
44 reveal different travel modes [7], travel demands [15,16], and the impact of social connections [17].  
45 These studies have provided strong supports for using LBSM data as proxies for studying mobility  
46 patterns of individuals and valuable insights into human mobility dynamics. However, the variations  
47 of movements in different spatial scales and temporal ranges are neglected in these studies, where  
48 the measurements of distances are either fixed in a certain time range or to a specific geographic  
49 region. For instances, the examinations on whether there are temporal (e.g., monthly or seasonal)  
50 changes within the movements or how the observed mobility patterns vary across different spatial  
51 scales (e.g., intra- or inter city or national levels) are lacking. Such insights are critical to advance  
52 our understandings of the collective mobility patterns for various applications, such as examining  
53 the mobility patterns across different cities [18], the spread patterns of disease [19,20] and touristic  
54 activities [12]. On the other hand, while the high-resolution spatiotemporal records from LBSM  
55 present unique research opportunities in this direction, the inherited large data volume poses  
56 significant data-intensive challenges for developing multi-scale spatiotemporal analysis approaches  
57 to dealing with the complexities in filtering movements of individuals, modeling and aggregating  
58 user trajectories at multiple spatial and temporal scales [21].

59 In this paper, we have employed a visual-analytics approach to exploring the Twitter user  
60 mobility patterns across multi-level spatial scales and temporal ranges in the continuous United States  
61 (i.e., excluding Alaska and Hawaii) during the year 2014. The mobility data is extracted from over 1.3  
62 billion geo-located Twitter messages (i.e., tweets) from 1<sup>st</sup> January to 31<sup>st</sup> December, 2014 over North  
63 America with over 6 million Twitter users and over 1 TB in file size. To address the data-intensive  
64 challenge embedded in this dataset, we have developed a scalable visual-analytics framework  
65 tailored to accommodate large volume of geo-located tweets. This framework is implemented  
66 based on high-performance distributed computing environment using Apache Hadoop<sup>1</sup>, which  
67 is an open source software framework to enable distributed processing of large datasets across  
68 computing clusters. Enabled by this framework, we have performed a set of statistical analysis  
69 to understand multi-scale spatiotemporal Twitter user mobility patterns. We have modeled the  
70 frequency of Twitter users visiting different locations to study the collective user visiting behaviors,  
71 where we have identified temporal similarities in the distributions. In particular, Twitter user mobility  
72 patterns measured by user displacements and radius of gyrations of individuals [6] have revealed  
73 different groups of Twitter users with multi-scale or multi-modal mobility patterns and multiple  
74 travel modes [7]. By further studying such mobility patterns in different temporal ranges, we have  
75 identified both consistency and seasonal fluctuations regarding the distance decay effects in the  
76 corresponding mobility patterns. In addition, our approach provides an interactive 3D virtual globe  
77 web mapping interface to enable exploratory geo-visual analytics for understanding the detailed  
78 Twitter user movement flows within a given spatial scale and time window.

---

<sup>1</sup> <http://hadoop.apache.org/>

The remainder of this paper is organized as follows. Section 2 describes the related work in the context of studying mobility patterns using LBSM data, in particular, the geo-located Twitter data. We focus on research challenges in using visual-analytics methods to enable multi-scale spatiotemporal analysis with massive movement datasets, including data management, multi-level spatiotemporal user trajectory modeling and visualization. Section 3 details the processes for extracting, aggregating and summarizing multi-level spatiotemporal Twitter user mobility patterns. Section 4 presents the case study of performing visual-analytics for seeking multi-scale spatiotemporal Twitter mobility patterns in the continuous United States of year 2014. Section 5 concludes the paper.

## 2. Mobility patterns in Location Based Social Media data

### 2.1. Geo-located Twitter data for studying large-scale user movements

To understand detailed mobility patterns of individuals, the capability to capture human movements with fine-grained spatial and temporal granularity is critical. In this connection, using GPS trackers tends to produce, to date, the most accurate records of individuals' movements regarding the accuracy of recorded user locations and update frequency [1]. However, such data are often limited in spatial scale (e.g., within a specific city or region) from a small group of people, for example, 226 and 182 volunteers participated in collecting such mobility data in [8] and [22] respectively. Other than tracking people directly, the vehicle-based GPS traces are often tied to specific vehicles (e.g. taxi), which are only accessible for a certain group of people [10].

Another approach from the literatures for studying human mobility is using mobile phone call data, such as Call Detail Records (CDR), where the locations of mobile users are estimated by cell tower triangulation with an accuracy in the order of kilometers [6,9,10]. Such a dataset can cover relatively large spatial scale [23,24] (e.g., national level) and a large portion of the population in the study region [10]. However, due to the concerns of infringement on individual privacy, mobile phone call data are not publicly accessible at all. Even such data were obtained in the mentioned studies, they came from various service providers covering different groups of users. These issues limit the capability for conducting reproducible scientific findings for mobility research, such as validating or extending the existing discoveries.

In this connection, it becomes increasingly popular for researchers to exploit the publicly accessible mobility data captured from today's pervasive Location Based Social Media (LBSM) platforms (e.g., Foursquare and Twitter). LBSM enables users to attach their current location as a geo-tag to the message they post, which is derived from either the GPS or Wi-Fi positioning with a high position resolution down to 10 meters [7]. A Big Data scenario emerges when millions social media users constantly post messages. In this study, geo-located Twitter data are chosen as a source for studying detailed mobility patterns. Compared to other LBSM platforms, Twitter is one of the most popular platforms and is been actively used in many countries. It provides a publicly accessible streaming API<sup>2</sup> for easy data access. Indeed, many other LBSM data can be collected from the data streams, such as Foursquare check-in data [16,25].

However, it is worth noting that there are some limitations and complexities in directly using LBSM data for studying human mobility patterns. For example, comparing to GPS traces, the update frequency of an individual's location varies depending on when a user is posting a new geo-located message or check-in at a new place. Although geo-located tweets tend to provide geo-locations with high position resolution as aforementioned [7], the information regarding the quality of the geo-locations is absent in each tweet. This will contribute to the uncertainties in calculating the distance of Twitter user movements, especially in densely built environments. There is also a potential mismatch regarding the representativeness of the overall population since not all people use social

<sup>2</sup> <https://dev.twitter.com/streaming/overview>

124 media or send geo-located messages [10], the demographic information of the Twitter users cannot  
125 be easily identified. The derived mobility patterns may lead to an over or under-representation  
126 of the real-world human mobility patterns. Many studies started to look into the demographic  
127 information of LBSM data, in particular Twitter data [26,27]. Although the used methods are still  
128 arguable, these issues certainly require us to pose stricter criteria in understanding human mobility  
129 patterns using geo-located Twitter data. On the other hand, geo-located Twitter dataset presents some  
130 unique advantages that make it a valuable proxy for studying human mobility patterns. For example,  
131 the high-resolution location information enables to identify multiple travel modes in user mobility  
132 patterns [7]; the large spatial coverage enables to study global mobility patterns [12], which is almost  
133 impossible for other mobility datasets. More importantly, by continuously monitoring the geo-located  
134 Twitter data streams with large volume of detailed and frequently updated spatiotemporal records  
135 of Twitter users, it offers a great deal of potential for studying mobility patterns of large groups of  
136 individuals at different spatial scales (e.g., movements across cities, states or even countries) and  
137 temporal gratuity (e.g., weekly, monthly, and seasonal movements), which is one of the motivations  
138 for this study.

## 139 2.2. Data-intensive challenges for multi-scale geo-visual analytics

140 Mobility data are essentially a collection of spatiotemporal records of people re-allocating across  
141 the geographic space. To study mobility patterns of individuals, a space-time trajectory of each  
142 individual user should be modeled and constructed to quantify the collective movements over  
143 space and time. Based on the extracted space-time trajectories, aforementioned studies are able  
144 to perform analysis, such as the measurements of user displacements and radius of gyrations of  
145 individuals, to study the mobility dynamics. Indeed, space-time trajectory is one of the core concepts  
146 in Hägerstrand's time geography to understand the embedded spatiotemporal dynamics [28],  
147 which has provided useful insights to explore movements across different geographical scales and  
148 temporal ranges. For example, a geo-visualization approach was used to study human activity  
149 patterns, where user trajectories were mapped in a 3D space ordered by timestamps in the third  
150 dimension [29]. While such an approach enables visualization of individual trajectories, its capability  
151 is limited in dealing with large-volume movement datasets [30]. Instead of directly visualizing  
152 an individual user's trajectories, a space-time cube approach was proposed to analyzing and  
153 visualizing the collective trajectories. It provides flexibilities in setting up both spatial scales and  
154 temporal ranges, and therefore is used to study mobility patterns across different spatial units (e.g.,  
155 countries, states, and cities, etc.) and identify the changes over space and time [31,32]. In this  
156 regard, visual-analytics methods are proposed to better convey the findings in terms of analyzing  
157 and visualizing multi-level spatiotemporal mobility patterns [30,33]. Visual-analytics methods  
158 focus on the synergy of computational and analytical methods to reduce the visual clutter, where  
159 aggregation methods are suggested to perform grouping/dividing individual's moving trajectories  
160 at different spatial and temporal granularity, e.g., utilizing the space-time cube approach [30].  
161 Employing visual-analytics methods dealing with massive movement datasets is not only beneficial  
162 for optimizing visualizations but also provides a great deal of flexibilities for performing statistical  
163 analysis in seeking mobility patterns with different level of spatiotemporal details.

164 However, in the context of studying mobility patterns using large volume of geo-located Twitter  
165 data, the inherited large data volume poses significant data intensive challenges for visual-analytics  
166 methods to scale with both the data volume and the computational requirements (e.g., movement  
167 extraction and trajectory modeling) [34]. In particular, in our study, 1.3 billion geo-located tweets  
168 were collected with over 1 TB in file size. To construct a space-time trajectory of an individual, it is  
169 necessary to go through the massive dataset to sort and update the trajectory whenever a new location  
170 is found. Such a task is already computationally demanding, let along breaking the trajectories  
171 to construct space-time cube with multiple spatial scale and temporal ranges. Indeed, developing  
172 a multi-scale spatiotemporal analysis approach is identified as one of the research challenges for

173 dealing with social media Big Data [21]. To address the data-intensive challenges, there is a need to  
174 develop a scalable visual-analytics framework tailored to accommodate large volume of geo-located  
175 tweets for studying multi-level spatiotemporal Twitter user mobility patterns.

### 176 3. Materials and Methods

#### 177 3.1. Geo-located Twitter data

178 Geo-located tweets are tweets appended with an additional geo-tag in the form of a pair  
179 of geographical coordinates, which represents the location a tweet was sent at. In this study,  
180 the geo-located tweets were downloaded using the Twitter Streaming API, where we specified a  
181 geographical bounding box as an area-of-interest to retrieve all the geo-located tweets that fall within  
182 it. To ensure complete coverage over the continuous United States, we implemented a crawler that  
183 selects North America as the initial area-of-interest, where the geographical boundary is specified  
184 with lower left (latitude: 5.4, longitude: -167.3) and upper right (latitude: 83.2, longitude: -52.2). The  
185 crawler is constantly running with over 2 million geo-located raw tweets (~2 GB in size) collected per  
186 day. We have collected more than 1.3 billion geo-located tweets from 1<sup>st</sup> January to 31<sup>st</sup> December,  
187 2014 with 6,147,430 Twitter users and 1 TB in file size. In particular, this data collection of year 2014  
188 was originally used to map the spatial spread of flu in North America during the time period [35].

189 As a social media account is not equal to a real person in the physical world [21], to ensure the  
190 data quality, the collected raw tweets were further filtered by the following steps: We first removed  
191 duplicated messages<sup>3</sup> in the dataset; and then we removed non-human users based on the heuristic  
192 of unusual relocating speed discussed in [7,12]. In this case, we adopted the speed limit value as  
193 240 m/s used in [7], where we examined all the consecutive locations of each user and excluded  
194 those with relocating speed over the limit. Note that the original location information embedded in  
195 each geo-located tweet is given in units of latitude and longitude, the distance is calculated by the  
196 great-circle distance between two points on a sphere with the haversine formula. Finally, we used the  
197 geographic boundaries of the continuous United States<sup>4</sup> (excluding Alaska and Hawaii) to further  
198 restrict the remaining tweets, where the technical details is presented in the following section. Based  
199 on these reinforcements, the dataset contains 1,052,861,000 tweets and 4,559,205 unique users.

#### 200 3.2. A scalable visual-analytics framework

201 To address the data-intensive challenges, we have developed a scalable visual-analytics  
202 framework tailored to accommodate large volume of geo-located tweets for studying multi-level  
203 spatiotemporal Twitter user mobility patterns. The scalable visual-analytics framework consists  
204 of two main units: (1) Data processing unit: a distributed computing environment using Apache  
205 Hadoop for modeling and extracting Twitter user movements, generating space-time user trajectories,  
206 and summarizing the movements at multiple spatiotemporal scales. (2) Geo-visualization unit:  
207 an interactive 3D virtual globe web mapping interface for exploratory geo-visual analytics for  
208 understanding the detailed Twitter user movement flows across different spatial scales and temporal  
209 ranges.

210 Apache Hadoop combines a distributed file system, namely Hadoop Distributed File  
211 System(HDFS) [36] with MapReduce programming paradigm [37], which can be applied to a  
212 wide range of data-intensive problems. Our framework benefits from using Hadoop in both data  
213 management and processing. First, since the input data is large it is desirable to store it on multiple  
214 machines. This provides scalability in relation to the growth of data size, where Hadoop can scale to  
215 more computing nodes in a cluster to maintain the performance. Second, by using Hadoop we can

<sup>3</sup> <https://support.twitter.com/articles/18311-the-twitter-rules>

<sup>4</sup> <https://www.census.gov/geo/maps-data/data/>

parallelize the computational tasks, where MapReduce breaks the entire computation into small tasks and schedule them among different computing nodes, to make the data processing faster and more efficient. An overall system architecture of the framework is shown in Figure 1. The details regarding the function and implementation of each unit are presented in the next sections.

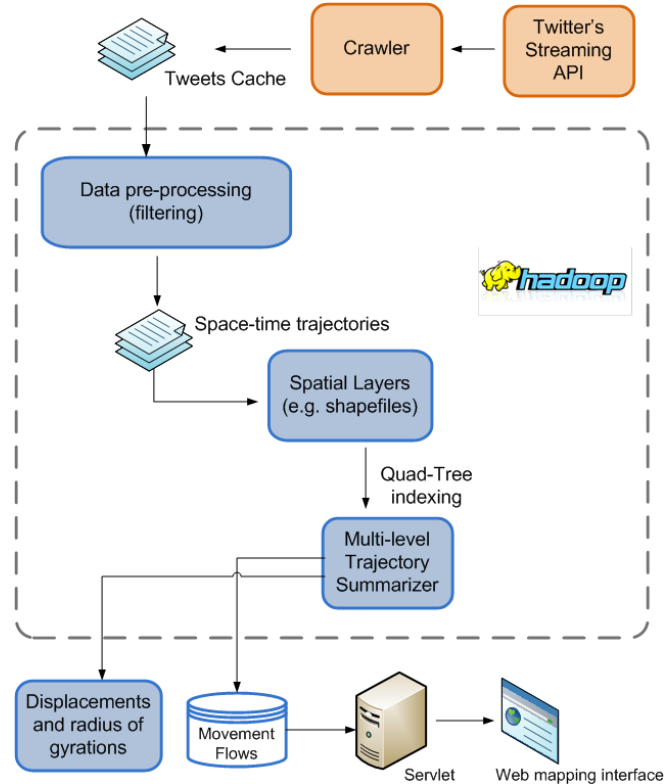


**Figure 1.** The overall system architecture of the framework

### 3.3. Space-time Twitter user trajectories

To derive meaningful mobility patterns of individuals, a space-time trajectory of each individual user should be constructed [28]. Each raw geo-located tweet contains multiple fields of information, such as the created time, country, language code, and location, etc. To construct a space-time trajectory from the data collection, we are interested in the following fields: *User ID*, *location*, *timestamp*, which can be represented by a tuple  $\langle id, loc, t \rangle$ , where *id* is a unique string representing a Twitter user's id; *loc* is the recorded location of the message represented as a pair of projected coordinates  $\langle x, y \rangle$ ; and *t* is the timestamp of when the message was posted; A Twitter user's space-time trajectory is defined as follows.

229

230 **Definition 1. Space-time Twitter user trajectory:** The space-time trajectory of a Twitter user is  
231 defined as a collection of recorded geo-locations in the chronological order (i.e., based on the attached  
232 timestamp):

233

$$234 \quad Trajectory_{user_id} \equiv \{ \langle id, loc_1, t_1 \rangle, \langle id, loc_2, t_2 \rangle, \langle id, loc_i, t_i \rangle, \dots \langle id, loc_n, t_n \rangle \}, i = 1, 2, 3 \dots n$$

235

236 To remove non-human users based on unusual relocating speed, a user will be removed  
237 if the speed between any two consecutive locations in the user's trajectory with speed  
238  $(loc_i - loc_{i-1}) > 240m/s$ . Based on this definition for modeling the space-time Twitter user  
239 trajectories, we converted the process of extracting trajectories from the raw geo-located Twitter data

240 as a MapReduce task. Specifically, each mapper utilizes the unique user id as a key to prepares the  
 241 records that belong to the same user and send them to a reducer. Once the reducers receive the  
 242  $\langle key, value \rangle$  pairs, a Twitter user's space-time trajectory is formed by the sorting the locations in  
 243 chronological order while considering the speed limit.

244  
 245 **Definition 2. Visitation behavior, displacement and radius of gyration:** As each space-time Twitter  
 246 user trajectory records all the locations a user has visited, the visitation behavior refers the frequency  
 247 of a user visiting different locations within a specific time frame. This metric provides an overall  
 248 assessment regarding the diversity and similarity in the collective mobility pattern [38].

249 In particular, the measurements of displacements and radius of gyrations of individuals are  
 250 two popular metrics to investigate and quantify the distance decay effects in the collective mobility  
 251 patterns [6]. The displacement refers to an individual's re-allocation across the geographic space  
 252 measured in distance, i.e.,  $distance(loc_i - loc_{i-1})$ . It is not equivalent to a "trip" took by an individual,  
 253 for instance, even the time interval between two recorded locations is one month, it will still count as  
 254 a displacement. By studying the collective displacements from a group people, it helps to identify  
 255 the distance bounds associated with different travel modes [7] and to quantitatively differentiate the  
 256 mobility patterns from random walks [5]. On the other hand, radius of gyration (donated as  $r_g$ ) is a  
 257 metric to distinguish mobility patterns of individuals [6], which is defined as follows.

$$258 \\ 259 r_g = \sqrt{\frac{1}{n} \sum_{i=1}^n (p_i - p_{centroid})^2}, \text{ where } p_{centroid} = \frac{1}{n} \sum_{i=1}^n p_i$$

260  
 261 It measures the accumulated distances of deviation from the center of mass of an individual user's  
 262 trajectory, and therefore indicates the individual's spatial coverage, where  $p_i$  and  $p_{centroid}$  are the  
 263  $i^{th}$  location and the geometric center of the user's trajectory, respectively. When applying the  
 264 measurement to the study population, it identifies different groups of people in terms of spatial  
 265 coverage from their corresponding mobility patterns. Note that both displacements and radius of  
 266 gyrations are measured by "crow's fly distance" in this study (i.e., the direct great-circle distance  
 267 between two recorded locations). Since these metrics are based on the generated trajectories,  
 268 by breaking and aggregating the trajectories in multiple spatial scales and temporal ranges, it  
 269 enables performing multi-scale spatiotemporal analysis on these measurements and studying the  
 270 corresponding mobility patterns.

### 271 3.4. Multi-level spatiotemporal trajectory aggregation

272 An important strategy for visual-analytics methods to deal with massive movement datasets is  
 273 performing spatial aggregations to provide different levels-of-detail [30,33]. It is similar to the map  
 274 generation approach that when a user is interacting with a map interface, the details of visualization  
 275 should be adaptive to a user's area-of-interest [39]. To enable aggregating Twitter trajectories into  
 276 multiple spatial scales, we have extended the hierarchical space-time cube model developed in [34],  
 277 where we partitioned the geographic space of the continuous United States into 10 hierarchical  
 278 spatial layers and each space-time cube is created with a fixed time window of a week interval.  
 279 Specifically, the state boundaries of the continuous United States are treated as the base layer (i.e.  
 280 level 0) for aggregating state-level Twitter user movements, Alaska and Hawaii are excluded for the  
 281 consideration of better visualization effects in the mapping interface of the framework. We then  
 282 created an hierarchical fishnet by diving the study region into regular cells, where the finest level  
 283 (level 10) consists  $1 \text{ km} \times 1 \text{ km}$  cells. Such a cell size is consistent with the spatial resolution in  
 284 landscan<sup>5</sup> product for measuring the global population density. In our case, the cell width/height  
 285 for level  $i-1$  is twice of the size in level  $i$ . Figure 2 illustrates an hierarchical fishnet spatial units

---

5 <http://web.ornl.gov/sci/landscan/>

for mapping multi-level Twitter user movements. Note that any predefined geographic boundaries can be used and appended in this framework to show different level-of-detailed movements (e.g., national-level and census-tract level), in our case, we replaced the level 8 fishnet layer with the US county boundaries.

To perform a multi-level spatial aggregation of the Twitter user trajectories using hierarchical spatial layers, each location in a user's trajectory is redistributed to the corresponding spatial units. A MapReduce algorithm for the spatial aggregation is implemented, where the ID of unit in each spatial layer (e.g., polygon in state and country layer and cell in the rest) is treated as key in the at the map stage. It performs a "point-in-polygon" geospatial operation to determine which polygon the point belongs to. If the location does not belong to any polygon, it will be dropped, which is how we used the geographic boundaries of the continuous United States to filter the raw tweet collection that initially covered the North America and kept the "domestic" ones. To optimize the "point-in-polygon" determination without comparing the location with every polygon in the spatial layer, we also created a Quad-Tree [40] for each spatial layer to speed up the process. Finally, the reducers generate two data outputs: (1) reconstructed space-time Twitter user trajectories at each spatial level (2) movement flows in the form of in and out movement flux between the spatial units. The movement flows are stored in the database for interactive explorations in the 3D web mapping interface, whereas the re-constructed trajectories can be further processed to produce distance measures at different spatial scales, which is illustrated as follows:

305

306  $Trajectory_{user_id} \equiv \{ \langle id, loc_1, t_1, unit_1 \rangle, \langle id, loc_2, t_2, unit_2 \rangle, \langle id, loc_i, t_i, unit_i \rangle, \dots \langle id, loc_n, t_n, unit_n \rangle \}$  where  
307  $i = 1, 2, 3 \dots n$

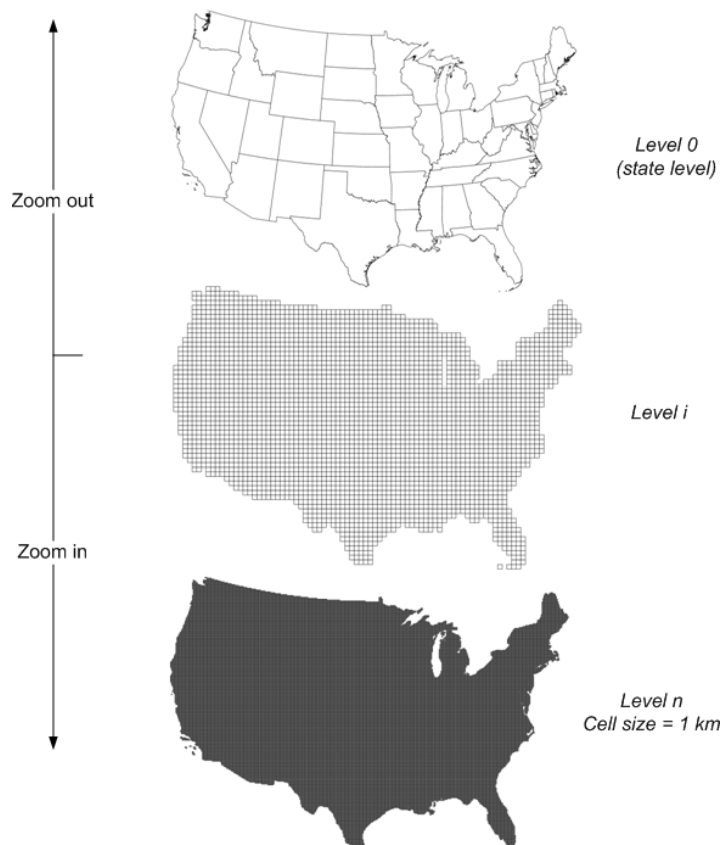


**Figure 2.** Hierarchical spatial layers for aggregating movements in different level-of-details

**308 4. Multi-scale spatiotemporal Twitter user mobility patterns****309 4.1. Spatiotemporal Twitter user mobility patterns**

310 The situation of using geo-located tweets as proxies to infer people's movements is complex as  
311 users' tweeting behavior can be significantly different from one to another, in particular, the frequency  
312 and time-interval between two consecutive tweets. For example, some people may tweet once a  
313 day while others do more; some people may tweet regularly while others do not. These tweeting  
314 behaviors are expected as such human dynamics are also seen in the mobile phone call data [6].  
315 Many studies have carried out data collection within a certain time period (e.g., a year in our case).  
316 However, as the geo-located tweets were collected in a continuous fashion, it is necessary to examine  
317 the sensitivities regarding these behaviors to ensure we are not just capturing a random snapshot  
318 from the whole data streams.

319 In this study, we have analyzed the cumulative distribution of the frequency Twitter users  
320 visiting different locations in year 2014 (and every month), which uses the methods developed in [41].  
321 The frequency is summarized based on the trajectories of individuals extracted from a monthly  
322 time span. Note that different groups of Twitter users may exist in each month. It appears that  
323 the distribution of the collective Twitter user visitation behaviors in year 2014 follows a two-tiered  
324 power law distributions (shown in Figure 3. The majority (the front part) of the distribution follows a  
325 truncated power-law distribution  $p(x) \sim x^{-\alpha} e^{-\lambda x}$ , where  $x$  is the number of visited locations and the  
326  $\alpha$  value is 1.32. The tail part (less than 2% of the whole population) follows a power-law distribution  
327  $p(x) \sim x^{-\alpha}$  with  $\alpha$  value is 3.5. This finding is consistent across all 12 months, with the mean  $\alpha$  value  
328 as  $1.34 \pm 0.05$  (standard deviation) and the mean  $\lambda$  value as  $0.00178 \pm 0.0002$  (standard deviation).

329 The two-tier power law distribution indicates that the collective behaviors of Twitter user  
330 visiting different locations can be well approximated with a (truncated) Lévy Walk model [8,42],  
331 which has also been identified in many human mobility studies using different mobility data [43].  
332 The similarities among the cumulative distributions suggest that the mobility data collected from  
333 geo-located tweets are temporally stable, at least at the monthly interval, which indicates the collected  
334 geo-located tweets in one month can potentially reveal similar findings as the ones collected in  
335 multiple months. In addition, the two-tier power law also reveals the diversity in the Twitter user  
336 visiting behaviors: (1) a small group Twitter users visited significantly more locations than the others  
337 (2) within each group, the probability of Twitter user visiting more locations decreases significantly  
338 with a power function.

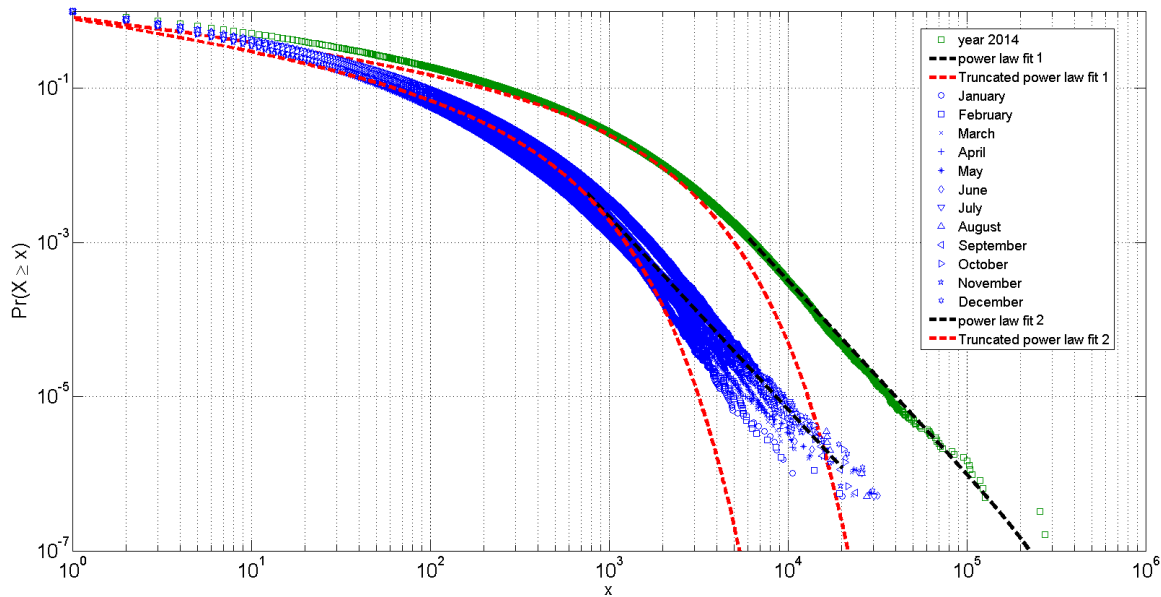


**Figure 3.** Two-tier power law distribution of the collective Twitter user visitation behaviors

As it is aforementioned, the measurements of displacements and radius of gyrations of individuals are two popular metrics to investigate and quantify the distance decay effects in the collective mobility patterns [6]. In this case, we first gathered the displacements from all the collected Twitter users in the continuous United States in year 2014, where those Twitter users with only one geo-located tweet were filtered out. To investigate the mobility patterns of individuals, we also derived the accumulated displacements and the radius of gyrations of each individual Twitter user based on the corresponding space-time trajectories over the one year period. Note that both displacements and radius of gyrations were calculated by the direct great-circle distance ( $d$ ) between two consecutively recorded locations in a user's trajectory.

To seek mobility patterns from these measurements, we performed statistical analysis regarding the probability distributions of displacements and radius of gyrations, which is also known as the spatial dispersal kernel  $P(d)$  [5]. The probability distribution of the user displacements (as well as accumulated displacements) is shown in Figure 4, whereas the probability distribution of radius of gyrations is shown in Figure 5. In this study, we used the fitting methods developed by [7]. The probability distributions of overall displacements, and the accumulated displacements and radius of gyrations of individuals, can all be approximated by a combination of three functions: an exponential function, a stretched-exponential function and a power-law function.

Figure 4 (a) shows the probability distribution of the overall displacements, which is approximated by  $P(d) \sim \lambda_1 e^{-\lambda_1(d-d_{min})}$ ,  $d_{min} = 10 \text{ m}$  from  $[10 \text{ m}, 70 \text{ m}]$  (accounting for 2 % of the population),  $P(d) \sim \beta \lambda_1 d^{\beta-1} e^{-\lambda^1(d^\beta-d_{min}^\beta)}$ ,  $d_{min} = 100 \text{ m}$  from  $[100 \text{ m}, 80 \text{ km}]$  (accounting for 93 % of the population), and  $P(d) \sim d^{-\alpha}$  ( $> 80 \text{ km}$ ) (accounting for 5 % of the population). In addition, the displacement in the distance bound from 100 m and 80 km in Figure 4 (b) can be further approximated by two power-law distributions with a cutting point at 5 km (53% distances are less than 5 km and 40% distances between 5 km and 80 km), which indicates two different travel modes, such as inter- or intra-city movements. Overall, the fitting functions with different distance bounds suggest the existence of multi-scale or multi-modal mobility patterns [7] of the Twitter users in the continuous United States, for example, the displacements larger than 80 km could be related to inter-state travels and stronger distance decay effects are observed in longer distance travels.

The probability distribution of radius of gyrations of individuals at the national level (Figure 5 (a)) is approximated by  $P(r_g) \sim \lambda_2 e^{-\lambda_2(r_g-r_{g_{min}})}$ ,  $r_{g_{min}} = 10 \text{ m}$  from  $[10 \text{ m}, 50 \text{ m}]$ ,  $P(r_g) \sim$

369  $\lambda_2 e^{-\lambda_2(r_g - r_{g_{min}})}$  from [50 m, 30 km], and  $P(r_g) \sim r_g^{-\alpha}$  [ $> 30$  km]. In particular, the radius of gyration  
 370 between 50 m and 30 km can be further approximately by two power law distributions with a cutting  
 371 point at 6 km (Figure 5 (b)), which suggest two main types of spatial coverage of from the collected  
 372 Twitter users in the continuous United States. The distribution shows that around 10% the tweet  
 373 population has a radius of gyration less than 50 meters, which indicates those twitter users mostly  
 374 tweet at a particular place, such as home or office; around 60% of the population has a radius of  
 375 gyration less than 30 km, which indicates that most of the collected Twitter user movements are  
 376 “short” distances, e.g., within a city locale. Note that the accuracy of these values for defining the  
 377 distance bound depends on the accuracy of the location information of each geo-located tweet.

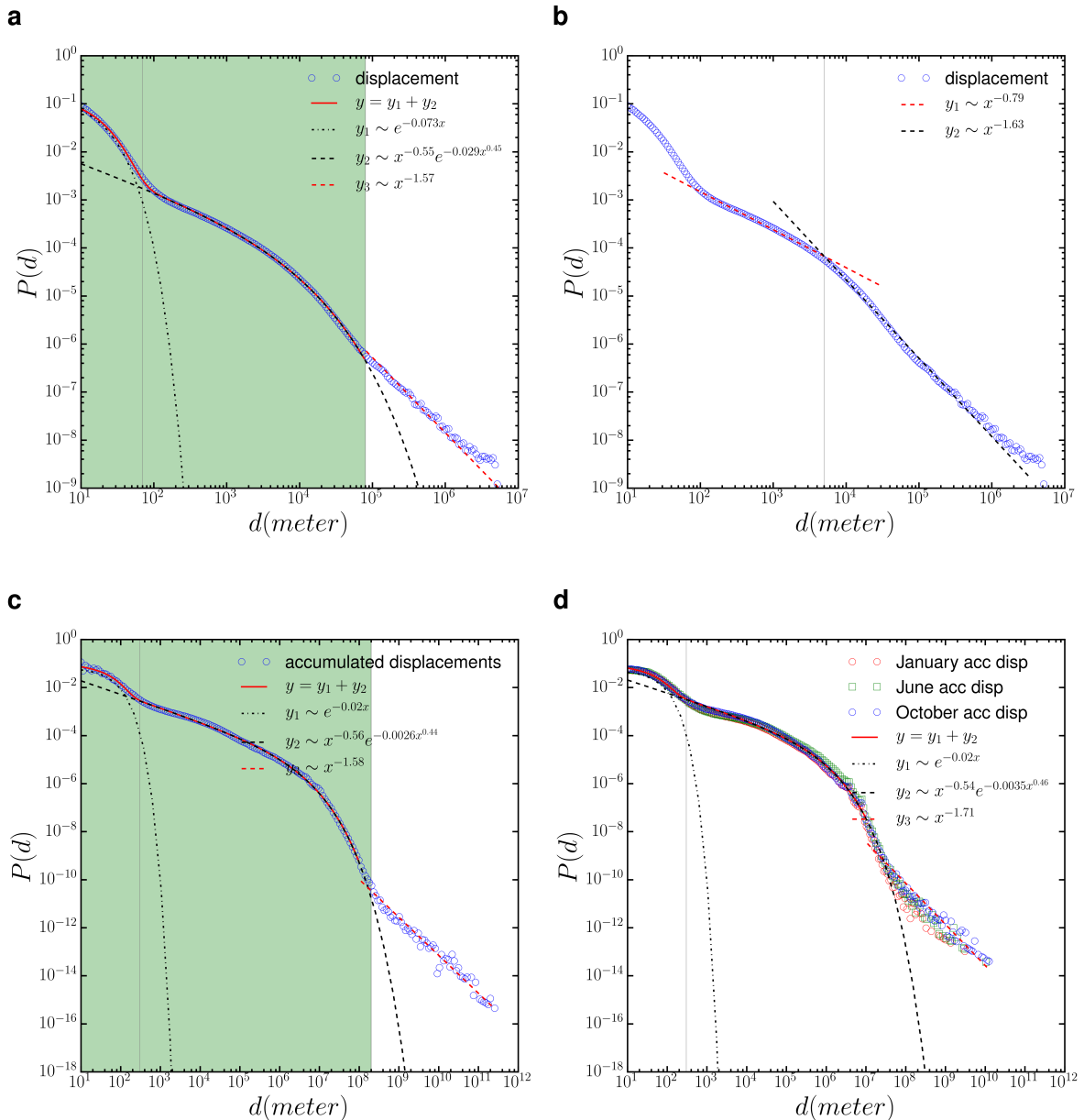


**Figure 4.** (a) The probability distribution of the collective Twitter user displacements  $P(d)$  (b) the distance between [100 m, 80 km] is approximated by a double power-law functions (c) The probability distribution of the accumulated displacements of individual Twitter users  $P(d)$  (d) The probability distribution of the accumulated displacements of individual Twitter users in 3 different months

We also measured the distribution of the radius of gyration of Twitter users at different spatial scales, specifically, the state level and city level. In this study, we selected the state Illinois and California for comparisons at the state level (Figure 5 (c)), whereas we chose Chicago city as an example (Figure 5 (d)) at the city level. Interestingly but not surprisingly, the  $P(r_g)$  at the state level can also be approximated by a combination of three functions: an exponential function, a stretched-exponential function and a power-law function. We noticed that distance bound of the radius of gyration at the state level is at 10 km instead of 30 km at the national level. The distance decay effects in larger spatial coverage [ $> 30$  km] slightly differ, in this case, the  $P(r_g)$  decreases faster in smaller size state (i.e., Illinois) than the large size state (i.e., California). In particular, the  $P(r_g)$  over Chicago city can be fitted by similar functions. However, as it reflects intra-city level mobility patterns, there is no distinct distance range to indicate large spatial coverage.

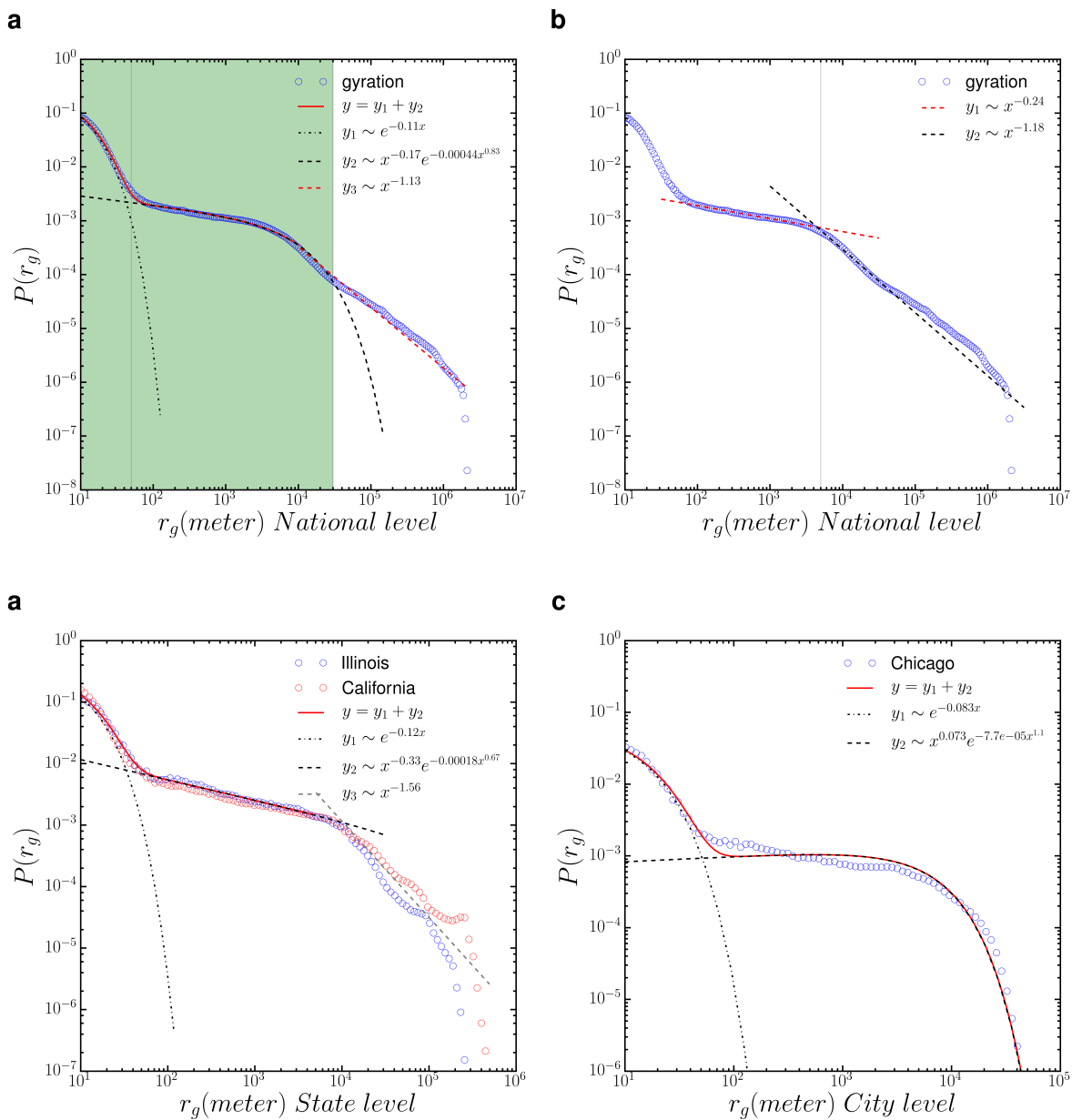


**Figure 5.** (a) The probability distribution of radius of gyration of individual Twitter users  $P(r_g)$  at the national level (b) the distance between [50 m, 30 km] is approximated by a double power-law functions (c)  $P(r_g)$  at the state level (Illinois and California) (d)  $P(r_g)$  for Chicago city

On the other hand, as our framework can aggregate Twitter user trajectories within different temporal ranges, we further analyzed the probability distributions of accumulated displacements took places in January, June, and October (Figure 4 (d)) and radius of gyrations within 4 quarters in year 2014 (Figure 6, in order to examine whether there are temporal changes in the mobility patterns. While the probability distributions of accumulated displacements are almost identical in those selected three months, we do find changes in the probability distributions of radius of gyrations in different quarters of the year. The fluctuations in the tails of the distributions indicate that long distance radius of gyrations (i.e., above 30 km) will experience more seasonal changes in the Twitter user mobility pattern, which means the increase or decrease of long distance movement activities in the corresponding time period. However, it is worthy noting that the overall trends in the Twitter user mobility patterns revealed by radius of gyrations are still consistent.

In summary, by comparing these results from different spatial scales and temporal ranges, different distance bounds were identified for describing the spatiotemporal Twitter user mobility patterns. However the overall similarity and consistence found in using a combination of three functions to approximate the probability distribution functions of displacements and radius of gyrations, clearly provide supports for using geo-located tweets as useful proxies for understanding human mobility patterns and conducting reproducible findings at multiple spatial scales and temporal ranges.

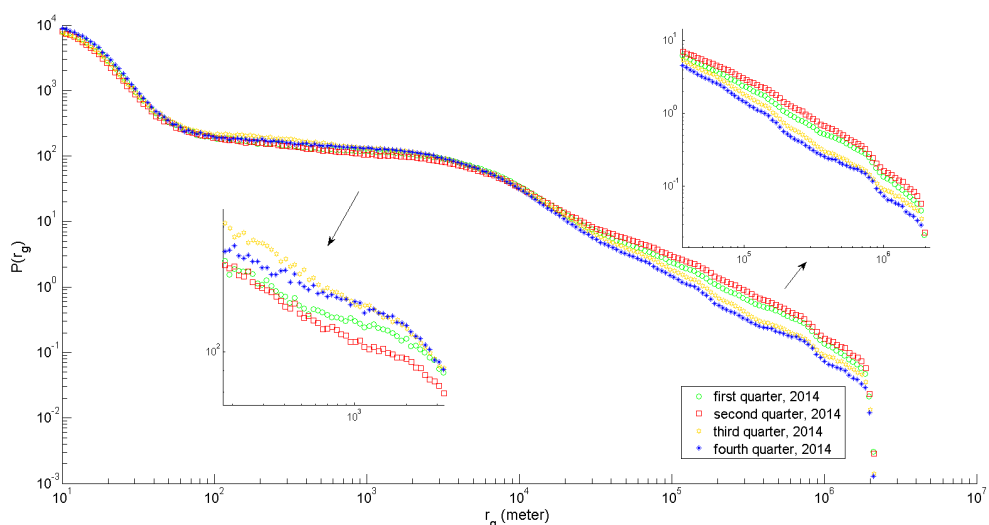


**Figure 6.** The probability distribution of radius of gyration of individual Twitter users in different quarters of year 2014

The above analysis of Twitter user mobility patterns mainly focuses on the spatiotemporal aspects. Our framework provides the flexibility to aggregate and extract Twitter user trajectories in a specific spatial scale and re-produce the analysis. In particular, as it is evident from the above analysis that there are multi-scale or multi-modal Twitter user mobility patterns, this framework can help further look into the mobility pattern regarding how Twitter users move across different spatial scales and temporal ranges, which is measured by the movement flows between these spatial units. The movement flows are obtained by aggregating the movements that started from and ended in the corresponding spatial units within the giving time frame. In this case, we demonstrate the inter-state mobility patterns by using the framework to capture the movement flows between the states. Note that the movement flows can be summarized across all the 10 spatial layers in the framework. We tested the overall distribution of the movement flows (in the form of weighted in-degree and out-degree of a graph, where each state is treated as a node) among different states in year 2014. We found that the probability distribution of Twitter user movement flows of visiting

420 different states follows a log-normal distribution:  $p(x) \sim \frac{1}{x} \exp\left[-\frac{(lnx-\mu)^2}{2\sigma^2}\right]$ , which suggests the flux  
 421 of Twitter user movements among the states are highly skewed and dominated by a few states. It  
 422 indicates that the Twitter population is not proportional to account the movement flux between the  
 423 states, which may provide some insights for other researchers in studying social-economical aspects  
 424 of the migration dynamics.

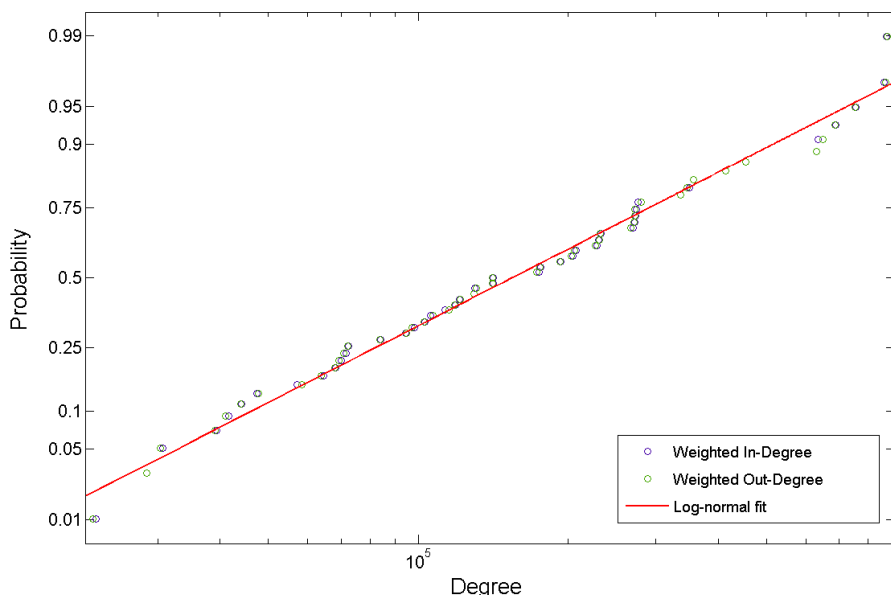


**Figure 7.** The distribution of Twitter user movement flows among different states in year 2014 measured in weighted in- and out-degrees

#### 425 4.2. The interactive 3D virtual globe web mapping interface

426 In addition to providing supports for understanding Twitter user mobility patterns with  
 427 statistical analysis, the framework integrates a 3D virtual globe interface to enable users to perform  
 428 exploratory geo-visual analytics of the multi-level spatiotemporal Twitter user movements<sup>6</sup>. The  
 429 3D virtual globe is developed and extended from the Cesium library<sup>7</sup>, which is an open-source  
 430 WebGL virtual globe and map engine. We customized the map engine to adapt different spatial  
 431 scales, which correspond to the hierarchical spatial layers, for aggregating movements in different  
 432 level-of-details. The map interface interprets user's interactions, such as area-of-interest, time  
 433 window, and zoom levels, etc. as parameters and send to the dedicated visualization servlet on the  
 434 CyberGIS Gateway, which is the leading online cyberGIS environment for a large number of users  
 435 to perform computing- and data-intensive, and collaborative geospatial problem-solving enabled by  
 436 advanced cyberinfrastructure [44].

437 An overview of the 3D web mapping interface is shown in Figure 8. The mapping interface  
 438 visualizes the corresponding movement flows on the virtual globe, where the number of movement  
 439 flows are divided by 20 percentiles and categorized by the colors shown in the legend. In terms  
 440 of performing exploratory visual-analytics of Twitter user movement patterns, users can specify the  
 441 time window to enable the query. When the results are shown, users can hover the mouse over  
 442 each individual lines on the map to see the value of movement flows for both in and out directions

<sup>6</sup> <http://sandbox.cigi.illinois.edu/home/apps.php?app=movepattern>

<sup>7</sup> <http://cesiumjs.org/>

(highlighted in color green). If the selected criteria keep unchanged, whenever the user zooms in/out, tilt or rotate the globe, the 3D virtual globe mapping interface will automatically provide the corresponding level-of-details on the fly. For example, Figure 9 and Figure 10 demonstrated the movement flows in different level-of-details around the Chicago city, and between O'Hare International Airport and the city center of Chicago city, where top 20 % movement flows were shown. The 3D mapping interface facilitates users to query multi-scale Twitter user movements with a geographical context and in an interactive fashion. For example, users can perform comparative studies of Twitter user movements in different cities by simply rotating the globe. More importantly, this mapping interface can be easily customized and extended to accommodate future geo-located Twitter data collection with larger spatial coverages. The source code of the visual-analytics framework in this paper is available upon request.

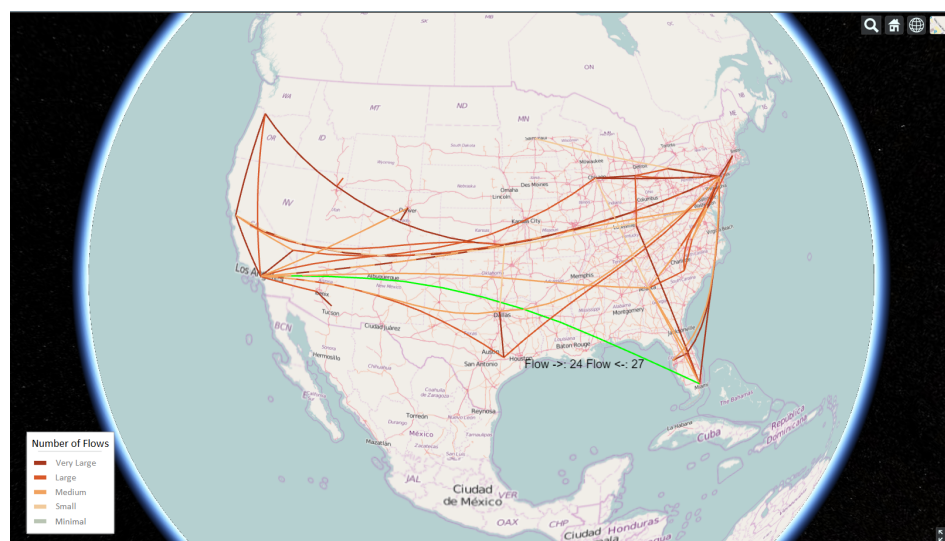


**Figure 8.** An overview of the 3D interactive web mapping interface

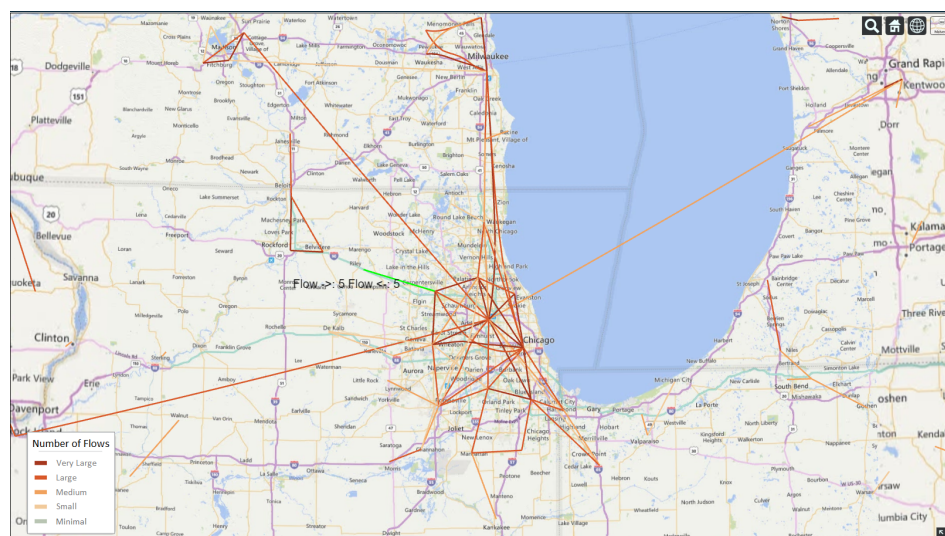


**Figure 9.** The top 20 % movement flows around Chicago city

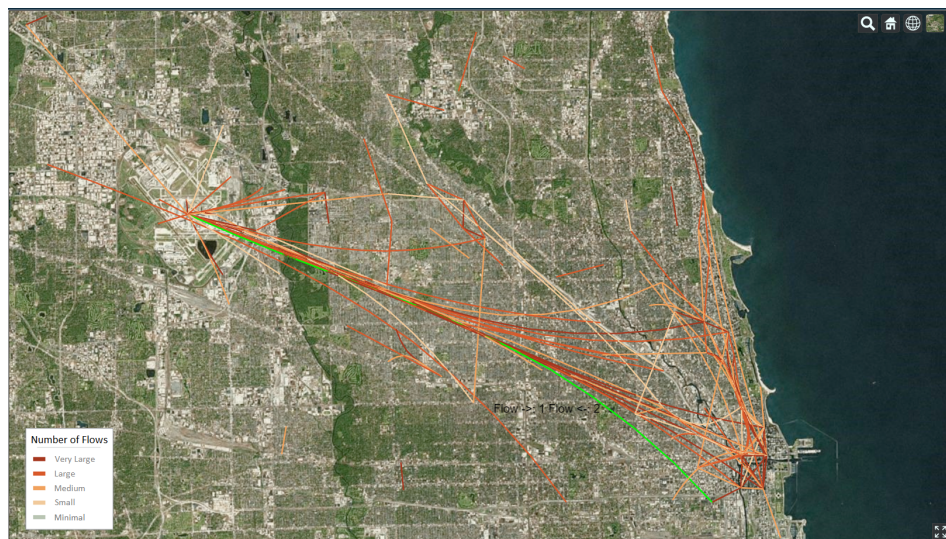


**Figure 10.** The top 20 % movement flows between O'Hare International Airport and the city center of Chicago city

## 454 5. Conclusions

455 In this study, we have used large volume of geo-located tweets to study Twitter user mobility  
 456 patterns across multi-level spatial scales and temporal ranges in the continuous United States during  
 457 the year 2014. To address the data-intensive challenges, we have developed a scalable visual-analytics  
 458 framework tailored to accommodate large volume of geo-located tweets for studying multi-scale  
 459 spatiotemporal Twitter user mobility patterns. This framework is implemented on high-performance  
 460 distributed computing environment using Apache Hadoop. It provides efficiency in filtering  
 461 large volume of geo-located tweets, modeling and extracting Twitter user movements, generating  
 462 space-time user trajectories, and summarizing multi-level spatiotemporal user mobility patterns. For  
 463 example, we have included an experiment for illustrating the processing time regarding generating  
 464 Twitter user trajectories across different time span in the supplement material.

465 With this framework, we have found some interesting Twitter user mobility patterns, both  
 466 statistically and visually. We studied the collective Twitter user visiting behavior regarding the  
 467 frequency of Twitter users visiting different locations, which was fitted by a two-tier power-law  
 468 distribution function. The two-tier power law distribution indicates that the collective behaviors  
 469 of Twitter user visiting different locations can be well approximated with a (truncated) Lévy Walk  
 470 model, which has also been identified in many human mobility studies using different mobility data.  
 471 The similarities among the cumulative distributions suggest that the mobility data collected from  
 472 geo-located tweets are temporally stable, at least at the monthly interval, which provides supports  
 473 that we are not just capturing a random snapshot of the whole data stream.

474 We studied the distance decay effects in the collective Twitter user movements measured  
 475 by the probability distributions of the displacements and radius of gyration of individuals.  
 476 These distributions can all be approximated by a combination of three functions: an exponential  
 477 function, a stretched-exponential function and a power-law function. In particular, distance bounds  
 478 between different fitting functions in displacement distribution reveals the existence of multi-scale  
 479 or multi-modal mobility patterns of the Twitter users, whereas the distribution of radius of gyration  
 480 reveals different groups of Twitter users with different types of spatial coverages at multiple spatial  
 481 scales. We further studied these mobility patterns in different temporal ranges to investigate the  
 482 temporal changes in the mobility patterns. We found that the accumulated displacements are almost  
 483 identical in different months, while the long distance radius of gyration (i.e., above 30 km) will  
 484 experience more seasonal changes in the Twitter user mobility pattern.

Finally, it is worth noting that at the current stage the geo-located Twitter data is not able to generalize to the entire population. As the demographic information of the Twitter users cannot be easily identified, the results derived in this study may not reflect a complete real-world image of human movements, which should be carefully considered in future studies. Nevertheless, the Twitter user movements provide clear supports to reveal the distance decay effects in human mobility research, which is observed in multiple spatial and temporal scales. Due to the large sample size, it is difficult to generalize the mobility pattern found at national level to entire population, city-level mobility pattern may provide better insights for investigating mobility dynamics. For example, the results of radius of gyration in Chicago exhibit similar pattern found in larger spatial scale, and with inputs of other mobility dataset that are often available at city-level, such as taxi trip records and mobile phone call data, there is a potential to synthesize these different sources of information and therefore provide a more complete image for understanding human mobility patterns. On the other hand, as we have discussed in this paper that geo-located Twitter data show the advantages regarding the easy data accessibility, the large spatial coverage and massive sample size, our approach took advantage of such data source to understand the mobility patterns across multiple spatial scales and temporal ranges. Also, our approach can be applied to the setting of other countries, which can be used to carry out comparative studies regarding spatiotemporal Twitter user mobility patterns.

**Acknowledgments:** The authors would like to thank the four anonymous reviewers of IJGI for their constructive comments that better shaped the paper. J.Y. would like to thank the funding support from the U.S. National Science Foundation under grant numbers: ACI-1047916, BCS-0846655, and IIS-1354329. D.Z. would like to thank the funding support from the Fundamental Research Funds for the Central Universities under grant number:2016XZZX004-02. The work also used the ROGER supercomputer, which is supported by NSF under grant number: 1429699.

**Author Contributions:** J.Y. conceived and designed the experiments; J.Y. and D.Z. wrote the paper.

**Conflicts of Interest:** The authors declare no conflict of interest. The founding sponsors had no role in the design of the study; in the collection, analyses, or interpretation of data; in the writing of the manuscript, and in the decision to publish the results.

## 512 Bibliography

- 513 1. Zheng, Y.; Li, Q.; Chen, Y.; Xie, X.; Ma, W.Y. Understanding mobility based on GPS data. Proceedings of  
514 the 10th international conference on Ubiquitous computing. ACM, 2008, pp. 312–321.
- 515 2. Jiang, B.; Yin, J.; Zhao, S. Characterizing the human mobility pattern in a large street network. *Physical  
516 Review E* **2009**, *80*, 021136.
- 517 3. Belik, V.; Geisel, T.; Brockmann, D. Natural human mobility patterns and spatial spread of infectious  
518 diseases. *Physical Review X* **2011**, *1*, 011001.
- 519 4. Greenwood, M.J. Human migration: Theory, models, and empirical studies. *Journal of regional Science*  
520 **1985**, *25*, 521–544.
- 521 5. Brockmann, D.; Hufnagel, L.; Geisel, T. The scaling laws of human travel. *Nature* **2006**, *439*, 462–465.
- 522 6. Gonzalez, M.C.; Hidalgo, C.A.; Barabasi, A.L. Understanding individual human mobility patterns.  
523 *Nature* **2008**, *453*, 779–782.
- 524 7. Jurdak, R.; Zhao, K.; Liu, J.; AbouJaoude, M.; Cameron, M.; Newth, D. Understanding Human Mobility  
525 from Twitter. *PLoS ONE* **2015**, *10*, e0131469.
- 526 8. Rhee, I.; Shin, M.; Hong, S.; Lee, K.; Kim, S.J.; Chong, S. On the levy-walk nature of human mobility.  
527 *IEEE/ACM transactions on networking (TON)* **2011**, *19*, 630–643.
- 528 9. Sevtsuk, A.; Ratti, C. Does urban mobility have a daily routine? Learning from the aggregate data of  
529 mobile networks. *Journal of Urban Technology* **2010**, *17*, 41–60.
- 530 10. Kung, K.S.; Greco, K.; Sobolevsky, S.; Ratti, C. Exploring universal patterns in human home-work  
531 commuting from mobile phone data. *PloS one* **2014**, *9*, e96180.
- 532 11. Thatcher, J. Living on fumes: Digital footprints, data fumes, and the limitations of spatial big data.  
533 *International Journal of Communication* **2014**, *8*, 1765–1783.
- 534 12. Hawelka, B.; Sitko, I.; Beinat, E.; Sobolevsky, S.; Kazakopoulos, P.; Ratti, C. Geo-located Twitter as proxy  
535 for global mobility patterns. *Cartography and Geographic Information Science* **2014**, *41*, 260–271.

- 536 13. Giannotti, F.; Pedreschi, D. *Mobility, data mining and privacy: Geographic knowledge discovery*; Springer  
537 Science & Business Media, 2008.
- 538 14. Crampton, J.W. Collect it all: national security, Big Data and governance. *GeoJournal* **2014**, pp. 1–13.
- 539 15. Wu, L.; Zhi, Y.; Sui, Z.; Liu, Y. Intra-urban human mobility and activity transition: Evidence from social  
540 media check-in data. *PloS one* **2014**, 9, e97010.
- 541 16. Hasan, S.; Zhan, X.; Ukkusuri, S.V. Understanding urban human activity and mobility patterns using  
542 large-scale location-based data from online social media. Proceedings of the 2nd ACM SIGKDD  
543 international workshop on urban computing. ACM, 2013, p. 6.
- 544 17. Cho, E.; Myers, S.A.; Leskovec, J. Friendship and mobility: user movement in location-based social  
545 networks. Proceedings of the 17th ACM SIGKDD international conference on Knowledge discovery and  
546 data mining. ACM, 2011, pp. 1082–1090.
- 547 18. Noulas, A.; Scellato, S.; Lambiotte, R.; Pontil, M.; Mascolo, C. A tale of many cities: universal patterns in  
548 human urban mobility. *PloS one* **2012**, 7, e37027.
- 549 19. Balcan, D.; Colizza, V.; Gonçalves, B.; Hu, H.; Ramasco, J.J.; Vespignani, A. Multiscale mobility networks  
550 and the spatial spreading of infectious diseases. *Proceedings of the National Academy of Sciences* **2009**,  
551 106, 21484–21489.
- 552 20. Tamerius, J.; Nelson, M.I.; Zhou, S.Z.; Viboud, C.; Miller, M.A.; Alonso, W.J. Global influenza seasonality:  
553 reconciling patterns across temperate and tropical regions. *Environmental health perspectives* **2011**, 119, 439.
- 554 21. Tsou, M.H. Research challenges and opportunities in mapping social media and Big Data. *Cartography  
555 and Geographic Information Science* **2015**, 42, 70–74.
- 556 22. Zheng, Y.; Xie, X.; Ma, W.Y. GeoLife: A Collaborative Social Networking Service among User, Location  
557 and Trajectory. **2010**.
- 558 23. Becker, R.; Cáceres, R.; Hanson, K.; Isaacman, S.; Loh, J.M.; Martonosi, M.; Rowland, J.; Urbanek,  
559 S.; Varshavsky, A.; Volinsky, C. Human mobility characterization from cellular network data.  
560 *Communications of the ACM* **2013**, 56, 74–82.
- 561 24. Sobolevsky, S.; Szell, M.; Campari, R.; Couronné, T.; Smoreda, Z.; Ratti, C. Delineating geographical  
562 regions with networks of human interactions in an extensive set of countries. *PLoS One* **2013**, 8, e81707.
- 563 25. Cranshaw, J.; Schwartz, R.; Hong, J.I.; Sadeh, N.M. The Livehoods Project: Utilizing Social Media to  
564 Understand the Dynamics of a City. ICWSM, 2012.
- 565 26. Mitchell, L.; Frank, M.R.; Harris, K.D.; Dodds, P.S.; Danforth, C.M. The geography of happiness:  
566 Connecting twitter sentiment and expression, demographics, and objective characteristics of place **2013**.
- 567 27. Longley, P.A.; Adnan, M.; Lansley, G.; others. The geotemporal demographics of Twitter usage.  
568 *Environment and Planning A* **2015**, 47, 465–484.
- 569 28. Hägerstrand, T.; others. Time-geography: focus on the corporeality of man, society, and environment.  
570 *The science and praxis of complexity* **1985**, pp. 193–216.
- 571 29. Kwan, M.P.; Lee, J. Geovisualization of human activity patterns using 3D GIS: a time-geographic  
572 approach. *Spatially integrated social science* **2004**, 27.
- 573 30. Andrienko, N.; Andrienko, G. Designing visual analytics methods for massive collections of movement  
574 data. *Cartographica: The International Journal for Geographic Information and Geovisualization* **2007**,  
575 42, 117–138.
- 576 31. MacEachren, A.M.; Kraak, M.J. Research challenges in geovisualization. *Cartography and Geographic  
577 Information Science* **2001**, 28, 3–12.
- 578 32. MacEachren, A.M. *How maps work: representation, visualization, and design*; Guilford Press, 2004.
- 579 33. Andrienko, G.; Andrienko, N.; Wrobel, S. Visual analytics tools for analysis of movement data. *ACM  
580 SIGKDD Explorations Newsletter* **2007**, 9, 38–46.
- 581 34. Cao, G.; Wang, S.; Hwang, M.; Padmanabhan, A.; Zhang, Z.; Soltani, K. A scalable framework for  
582 spatiotemporal analysis of location-based social media data. *Computers, Environment and Urban Systems*  
583 **2015**, 51, 70–82.
- 584 35. Padmanabhan, A.; Wang, S.; Cao, G.; Hwang, M.; Zhang, Z.; Gao, Y.; Soltani, K.; Liu, Y. FluMapper:  
585 A cyberGIS application for interactive analysis of massive location-based social media. *Concurrency and  
586 Computation: Practice and Experience* **2014**.
- 587 36. Shvachko, K.; Kuang, H.; Radia, S.; Chansler, R. The hadoop distributed file system. *Mass Storage  
Systems and Technologies (MSST)*, 2010 IEEE 26th Symposium on. IEEE, 2010, pp. 1–10.

- 589 37. Dean, J.; Ghemawat, S. MapReduce: simplified data processing on large clusters. *Communications of the*  
590 *ACM* **2008**, *51*, 107–113.
- 591 38. Gao, H.; Tang, J.; Liu, H. Exploring Social-Historical Ties on Location-Based Social Networks. ICWSM,  
592 2012.
- 593 39. Buttenfield, B.P.; McMaster, R.B. *Map Generalization: Making rules for knowledge representation*; Longman  
594 Scientific & Technical New York, 1991.
- 595 40. Samet, H. The quadtree and related hierarchical data structures. *ACM Computing Surveys (CSUR)* **1984**,  
596 *16*, 187–260.
- 597 41. Clauset, A.; Shalizi, C.R.; Newman, M.E. Power-law distributions in empirical data. *SIAM review* **2009**,  
598 *51*, 661–703.
- 599 42. Reynolds, A. Truncated Lévy walks are expected beyond the scale of data collection when correlated  
600 random walks embody observed movement patterns. *Journal of The Royal Society Interface* **2012**, *9*, 528–534.
- 601 43. Zhao, K.; Musolesi, M.; Hui, P.; Rao, W.; Tarkoma, S. Explaining the power-law distribution of human  
602 mobility through transportation modality decomposition. *Scientific reports* **2015**, *5*.
- 603 44. Liu, Y.; Padmanabhan, A.; Wang, S. CyberGIS Gateway for enabling data-rich geospatial research and  
604 education. *Concurrency and Computation: Practice and Experience* **2014**.

605 © 2016 by the authors. Submitted to *ISPRS Int. J. Geo-Inf.* for possible open access publication under the terms  
606 and conditions of the Creative Commons Attribution license (<http://creativecommons.org/licenses/by/4.0/>)